JOC*Article*

Synthesis and Application of Chiral Cyclopropane-Based Ligands in Palladium-Catalyzed Allylic Alkylation

Gary A. Molander,* Jason P. Burke, and Patrick J. Carroll†

Roy and Diana Vagelos Laboratories, Department of Chemistry, University of Pennsylvania, Philadelphia, Pennsylvania 19104-6323

gmolandr@sas.upenn.edu

Received July 16, 2004

A series of chiral, cyclopropane-based phosphorus/sulfur ligands have been synthesized and evaluated in the palladium-catalyzed allylic alkylation of 1,3-diphenylpropenyl acetate with dimethyl malonate. Variation of the ligand substituents at phosphorus, sulfur, and the carbon backbone revealed **24d** to have the optimal configuration for this reaction, giving the product in high yield and with good enantioselectivity (93%). A model for the observed enantioselectivity is discussed within the context of existing models, using X-ray crystallographic data, solution-phase NMR studies, and the absolute stereochemistry of the products. Selected ligands were also evaluated in the palladium-catalyzed intermolecular Heck reaction and the rhodium-catalyzed hydrogenation of a dehydroamino acid.

Introduction

The asymmetric catalysis of organic reactions to provide enantiomerically enriched compounds has became one of the most powerful tools in modern synthetic organic chemistry.[1] The majority of recent progress in this field has come from metal complexes containing chiral organic ligands. A quick survey of the most efficient ligands, however, reveals an interesting fact: most belong to just a few structural classes. This is true whether referring to the C_2-symmetric diphosphine ligands that originally dominated the field or to the more recently introduced bidentate ligands with mixed coordinating atoms. Examples of the former include binaphthyl and biaryl derivatives, bisoxazolines, salens, and tartrate-based ligands, all of which are C_2-symmetric. Examples of the latter include those derived from ferrocenylphosphines, phosphinooxazolines, and cinchona alkaloids.

Until a method exists for the accurate and reliable rational design of ligands, an empirical exploration of various ligand frameworks and chelating atoms remains one of the best ways to discover new catalyst systems. Although a large variety of structurally diverse ligands have already been tested in asymmetric catalysis, cyclopropane skeletons have received relatively little attention to date. This is surprising because the cyclopropane ring offers an advantageous combination of structural rigidity, low molecular weight on a well-defined and highly variable platform, and unusual bond angles. Moreover, recent improvements in the stereoselective synthesis of this ring make exploring the use of cyclopropanes even more attractive.[2,3]

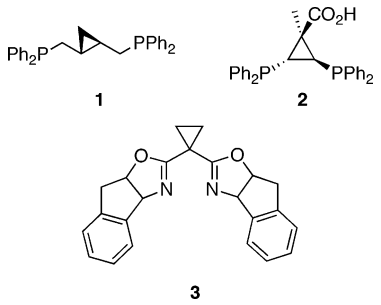

FIGURE 1. Cyclopropane-based chiral ligands.

The first appearance of a cyclopropane-based ligand in the literature was in 1979, by Colleuille and co-workers (**1**, Figure 1).[4] In a survey of several other ring structures, a cyclopropyl-based diphosphine ligand was tested in the rhodium-catalyzed hydrogenation of dehydroamino acids, providing a 23% ee of the reduction product.

In 1992, Minami and co-workers evaluated diphosphine **2** in an asymmetric allylic alkylation catalyzed by palladium, and in this case a 61% ee was achieved.[5] More recently, Sibi and co-workers have used bisoxazoline **3** in a variety of different transformations with excellent enantioselectivity. In these latter studies, however, advantage was not taken of the unique structural features of the cyclopropyl moiety in orienting the heteroatoms bound to the metal.[6,7]

† To whom all correspondence concerning X-ray crystal structures should be addressed.

(1) *Comprehensive Asymmetric Catalysis*; Jacobsen, E. N., Pfaltz, A., Yamamoto, H., Eds.; Springer-Verlag: Berlin, Germany, 1999.

(2) Lebel, H.; Marcoux, J. F.; Molinaro, C.; Charette, A. B. *Chem. Rev.* **2003**, *103*, 977−1050.

(3) *Comprehensive Asymmetric Catalysis*; Jacobsen, E. N., Pfaltz, A., Yamamoto, H., Eds.; Springer-Verlag: Berlin, Germany, 1999; Vol. 2, pp 513−606.

(4) Aviron-Violet, P.; Colleuille, Y.; Varagnat, J. *J. Mol. Catal.* **1979**, *5*, 41−50.

(5) Okada, Y.; Minami, T.; Yamamoto, T.; Ichikawa, J. *Chem. Lett.* **1992**, 547−50.

(6) Sibi, M. P.; Ji, J. *J. Org. Chem.* **1997**, *62*, 3800−3801.

10.1021/jo048782s CCC: $27.50
Published on Web 10/19/2004

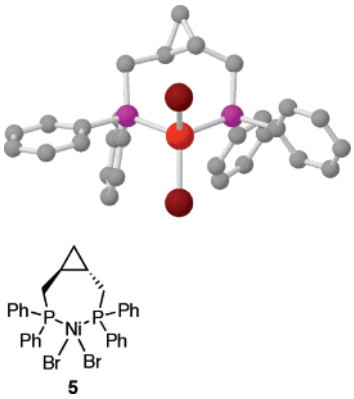

FIGURE 2. X-ray crystal structure of Ni(**1**)Br_2.

We sought to explore the three-dimensional space of the cyclopropyl motif in greater depth to determine its potential utility in asymmetric synthesis, and some of our initial results are reported herein.

Results and Discussion

As an easy entry into cyclopropane-based catalysts and a useful point of reference for further studies, ligand **1** was synthesized with use of the known alcohol **4** (eq 1).[8]

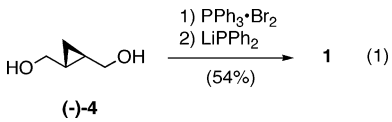

As might have been anticipated, when tested in the palladium-catalyzed allylic alkylation of 1,3-diphenylpropenyl acetate with dimethyl malonate, ligand **1** produced disappointing results in a variety of solvents (25−27% ee). To gain insight into why ligand **1** performed so poorly, metal complexes were synthesized for X-ray analysis.

The solid-state structures clearly show that although ligand **1** is indeed able to chelate tetrahedral nickel(II) (with a bite angle of 105.4°), the square-planar geometry of palladium(II) results in a dimeric complex with bridging ligands (Figures 2 and 3). This suggests that the active catalyst in the allylic alkylation reaction and the reduction reactions of Colleuille et al. are actually dimeric or a mixture of monomeric nonchelated catalyst complexes, resulting in a highly fluxional environment that subsequently leads to lower enantioselectivity.

First-Generation P/S Ligands. With these results in mind, new frameworks were designed with more accommodating metal-chelating centers. The systems initially chosen (**10** and **12**, Scheme 1) bore a cis orientation of heteroatoms to facilitate chelation and were accessed via a modular approach that allowed fine-tuning of ligand performance. The smaller chelate ring required the use of electronic effects to direct the incoming nucleophile and thereby control asymmetric induction, as opposed to restricting the number of diastereomeric transition states via the C_2-symmetrical paradigm inef-

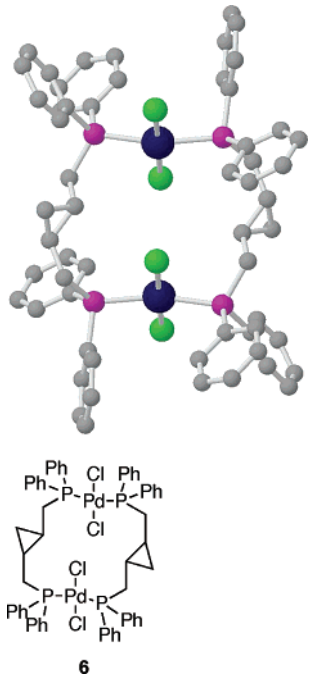

FIGURE 3. X-ray crystal structure of [Pd(**1**)Cl_2]$_2$.

fectively incorporated within the first model system. Though many combinations of strong and weak heteroatom pairs are known, several recent reports demonstrating the utility of P/S ligands in a variety of different applications made it an appealing choice.[9−17]

The first generation of P/S ligands took advantage of the known iodo alcohol **7**, derived from a Charette cyclopropanation (Scheme 1).[18]

Variations in the carbon framework were also explored, although the *gem*-dimethyl analogue required a resolution to obtain enantiopure ligand (Scheme 2).

For comparison, a 1,2-trans substituted ligand (**17**) was also synthesized (Scheme 3).

The ligands were then tested according to the standard palladium-catalyzed asymmetric allylic alkylation (AAA) with 1,3-diphenylpropenyl acetate and dimethyl malonate (Table 1). The ee values were reported as observed (uncorrected) for ligands of ~90% ee (**10**, **12**, and **17**) or 99% ee (**15**). Results show that having the phosphorus directly attached to the cyclopropane ring was beneficial (**12** versus **10**), but altering the carbon framework (**12f** versus **15**) or the cis configuration of the cyclopropane

(7) Sibi, M. P.; Ma, Z.; Jasperse, C. P. *J. Am. Chem. Soc.* **2004**, *126*, 718−719.
(8) Barrett, A. G. M.; Hamprecht, D.; White, A. J. P.; Williams, D. J. *J. Am. Chem. Soc.* **1997**, *119*, 8608−8615.
(9) Albinati, A.; Eckert, J.; Pregosin, P.; Ruegger, H.; Salzmann, R.; Stossel, C. *Organometallics* **1997**, *16*, 579−590.
(10) Enders, D.; Peters, R.; Runsink, J.; Bats, J. W. *Org. Lett.* **1999**, *1*, 1863−1866.
(11) Evans, D. A.; Campos, K. R.; Tedrow, J. S.; Michael, F. E.; Gagne, M. R. *J. Am. Chem. Soc.* **2000**, *122*, 7905−7920.
(12) Yan, Y. Y.; RajanBabu, T. V. *Org. Lett.* **2000**, *2*, 199−202.
(13) Nakano, H.; Okuyama, Y.; Yanagida, M.; Hongo, H. *J. Org. Chem.* **2001**, *66*, 620−625.
(14) Sugama, H.; Saito, H.; Danjo, H.; Imamoto, T. *Synthesis* **2001**, 2348−2353.
(15) Mancheno, O. G.; Priego, J.; Cabrera, S.; Arrayas, R. G.; Llamas, T.; Carretero, J. C. *J. Org. Chem.* **2003**, *68*, 3679−3686.
(16) Faller, J. W.; Wilt, J. C.; Parr, J. *Org. Lett.* **2004**, *6*, 1301−1304.
(17) Nakamura, S.; Fukuzumi, T.; Toru, T. *Chirality* **2004**, *16*, 10−12.
(18) Charette, A. B.; Juteau, H.; Lebel, H.; Molinaro, C. *J. Am. Chem. Soc.* **1998**, *120*, 11943−11952.

SCHEME 1

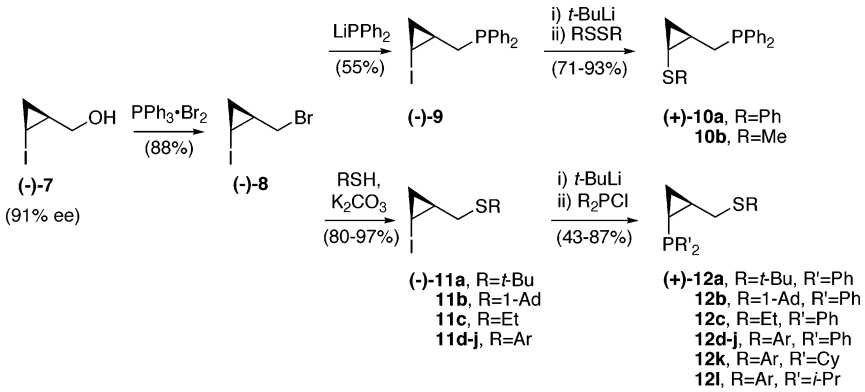

SCHEME 2[a]

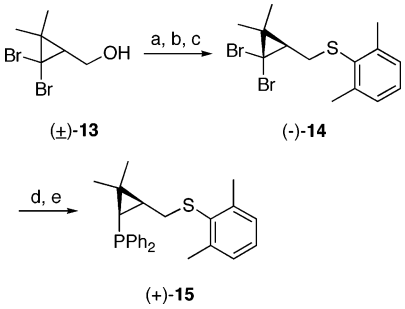

[a] Reagents and conditions: (a) (+)-3-bromocamphor-8-sulfonic acid chloride, Et_3N; (b) resolve; (c) 2,6-$(Me)_2$PhSH, K_2CO_3, DMF, 86%; (d) Zn, AcOH, 6:1 dr, 38%; (e) *t*-BuLi; Ph_2PCl, 60%.

SCHEME 3[a]

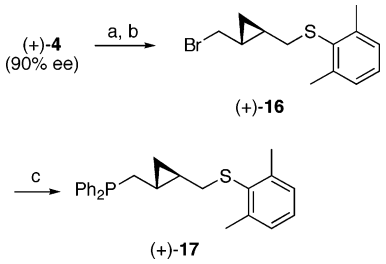

[a] Reagents and conditions: (a) PPh_3, Br_2, 63%; (b) 2,6-$(Me)_2$PhSH (1 equiv), K_2CO_3, DMF, 43%; (c) $LiPPh_2$, 61%.

(e.g., to *trans*-**12f** and **17**) was not. Additionally, bulky aromatic substituents on the sulfur gave the best results (**12f**), with electron-donating groups giving improved yield and enantioselectivity (**12g** versus **12h**). However, increasing the steric bulk on the sulfide aromatic ring did not always increase the enantioselectivity (**12j**). Varying substituents on the phosphine did not show any improvement either (**12k**,***l***).

X-ray Structures. Solid-state structures confirmed that the cis ligands did indeed chelate without forming dimers (Figures 4−6). The trans influence could also be seen, with the Pd−Cl bond trans to phosphorus measuring 0.06 Å longer than the corresponding bond trans to sulfur for complex **18** (Figure 4). The triisopropyl complex **19** was relatively similar in both bite angle and magnitude of the trans influence (Figure 5), while **20** showed a smaller difference in the trans effect (0.04 Å). Additionally, while complexes **18** and **19** showed a twist boat conformation, the *gem*-dimethyl complex **20** was essentially planar (Figure 6). On this basis, there is no obvious, direct correlation between either the effective trans effect or the conformation of the chelate with the ee values observed.

TABLE 1. Best Results of P/S Ligands Tested in Pd-Catalyzed AAA

L*	R	R′	ee, %
10a[a]	Ph	Ph	22
10b[a]	CH_3	Ph	23
12a	Ph	*t*-Bu	70
12b	Ph	1-Ad	69
12c	Ph	Et	76
12d[b]	Ph	Ph	48
12e	Ph	3,5-$(Me)_2$Ph	59
12f	Ph	2,6-$(Me)_2$Ph	78
trans-**12f**	Ph	2,6-$(Me)_2$Ph	33
12g	Ph	4-(CF_3)Ph	48
12h	Ph	4-(MeO)Ph	65
12i	Ph	2,4,6-$(Me)_3$Ph	74
12j[b]	Ph	2,4,6-(*i*-Pr)$_3$Ph	72
12k[c]	Cy	2,6-$(Me)_2$Ph	76
12*l*[a]	*i*-Pr	2,6-$(Me)_2$Ph	64
15	Ph	2,6-$(Me)_2$Ph	24
17	Ph	2,6-$(Me)_2$Ph	16

[a] THF used as solvent. [b] Toluene used as solvent. [c] CH_2Cl_2 used as solvent.

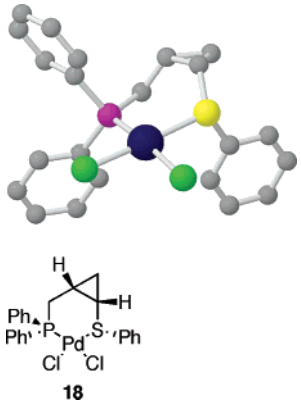

FIGURE 4. X-ray crystal structure of Pd(**10a**)Cl_2.

Second-Generation P/S Ligands. Although these P/S ligands represented a drastic improvement upon the

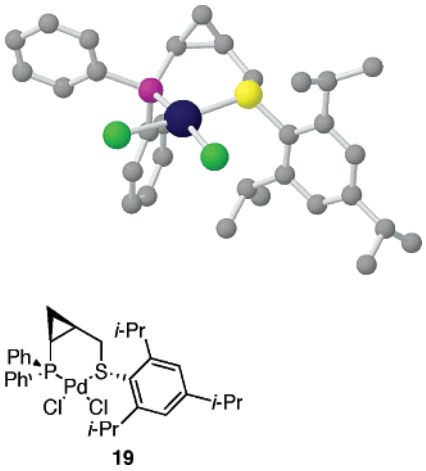

FIGURE 5. X-ray crystal structure of Pd(**12j**)Cl_2.

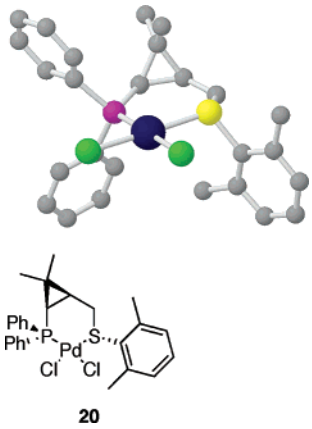

FIGURE 6. X-ray crystal structure of Pd(**15**)Cl_2.

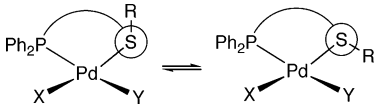

FIGURE 7. Isomerization of the *S*-stereocenter upon metal coordination.[11]

initially tested ligand **1**, a second series of P/S ligands was designed to overcome some of the weaknesses inherent in the first-generation design (ligands **10**, **12**, **15**, and **17**). By placing an additional stereocenter between the sulfide and the cyclopropane ring, we perceived that two key problems of the first-generation ligands could be solved: (1) iodo alcohol **7** was generated in ≤90% ee, which, neglecting any nonlinear effects, thereby limited the potential enantiopurity of the catalyzed reaction products, and (2) inversion of stereochemistry at the newly formed stereogenic site at sulfur upon coordination with the metal created the possibility of isomerization and the generation of competing diastereomeric complexes (Figure 7).[19]

Synthesis of the second-generation ligands began with the commercially available (*R*)-3-butyn-2-ol (>98% ee) that was easily iodinated and reduced with diimide (Scheme 4). The vinyl iodide was then diastereoselectively cyclopropanated to afford a single isomer by NMR analysis. The selectivity of this reaction is rationalized by steric strain in the transition structure as a result of $A^{1,3}$-interactions. The relative stereochemistry of **22** was determined by X-ray crystallographic analysis of the *p*-bromobenzoyl ester derivative.

SCHEME 4[a]

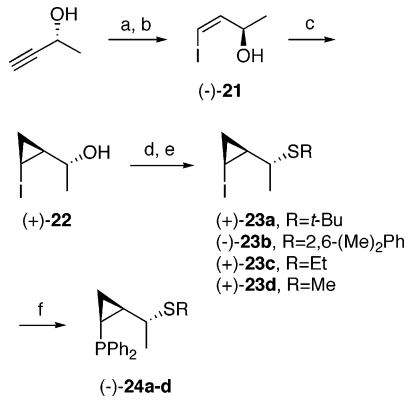

[a] Reagents and conditions: (a) *n*-BuLi; I_2, 98%; (b) $KO_2CN{=}N$-CO_2K, AcOH, 87%; (c) Et_2Zn, CF_3CO_2H, CH_2I_2, 74%; (d) PPh_3, Br_2, 5:1 dr, 91%; (e) RSH, Cs_2CO_3, 35−87%; (f) *t*-BuLi, Ph_2PCl, 45−84%.

TABLE 2. Best Results of Second Generation P/S Ligands in Pd-Catalyzed AAA

L*	Pd	yield, %	ee, %
24a	$[Pd(allyl)Cl]_2$	78	75
24a·BH_3	$Pd(OAc)_2$	>95	44
24b	$[Pd(allyl)Cl]_2$	>95	74
24b·BH_3	$Pd(OAc)_2$	>95	64
24c	$[Pd(allyl)Cl]_2$	>95	91
24d	$[Pd(allyl)Cl]_2$	>95	93

The standard palladium-catalyzed AAA utilized to benchmark this second generation of ligands provided much more promising results (Table 2). Surprisingly, the smaller sulfide substituents clearly gave the best results, with the *S*-methyl ligand **24d** affording the best enantioselectivity of all ligands tested in this study. This was counterintuitive based upon the known inversion of sulfides chelating to metals and the resulting preponderant use of bulky alkyl groups employed in most successful P/S ligands to prevent this phenomenon.[11,12,15,17,20] Subjecting the borane-protected ligands (**24a**·BH_3, **24b**·BH_3) to the same reaction conditions with $Pd(OAc)_2$, forming palladium(0) in situ, reduced both the rate and the enantioselectivity of the reaction.[21]

To our chagrin, the *S*-methyl ligand **24d** was the most difficult to prepare, because only by using a nucleophile prepared in situ from methanethiol (a gas at room temperature) could success be achieved in incorporation of the thioalkoxy group. All other attempts at its syn-

(19) Murray, S. G.; Hartley, F. R. *Chem. Rev.* **1981**, *81*, 365−414.

(20) Albinati, A.; Pregosin, P. S.; Wick, K. *Organometallics* **1996**, *15*, 2419−2421.

(21) Riegel, N.; Darcel, C.; Stephan, O.; Juge, S. *J. Organomet. Chem.* **1998**, *567*, 219−233.

TABLE 3. Results of Ligand 24d with Various Nucleophiles and Electrophiles in Pd-Catalyzed AAA

electrophile	nucleophile	product	solvent	% yield	% ee
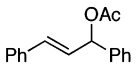	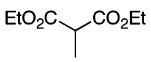	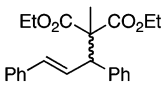	CH_2Cl_2	>95	81
			THF	>95	84
			MeCN	>95	76
"	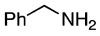	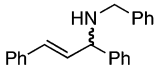	CH_2Cl_2	36	77
			THF	5	72
			MeCN	71	86
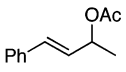	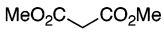	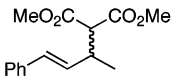	CH_2Cl_2	>95	31
			THF	>95	33
			MeCN	>95	23
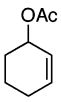	"	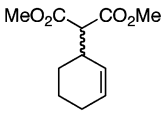	CH_2Cl_2	90	14
			THF	75	16
			MeCN	<5	-

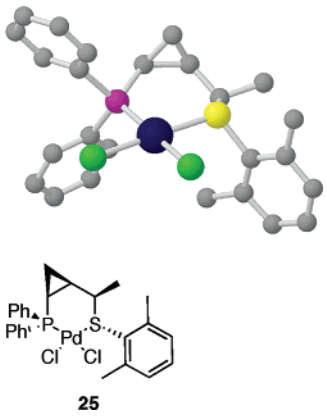

25

FIGURE 8. X-ray structure of Pd(**24b**)Cl_2.

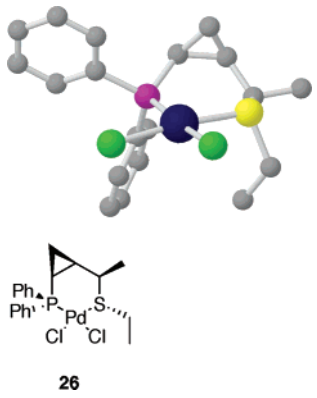

26

FIGURE 9. X-ray structure of Pd(**24c**)Cl_2.

thesis failed, whether using previously deprotonated methanethiol or forming the thiolate in situ through reduction of the disulfide. Nevertheless, **24d** could be obtained in quantities suitable for further studies.

Scope. Ligand **24d** was evaluated in other AAA reactions with various electrophiles and nucleophiles to determine the scope of its performance (Table 3). Disappointingly, ligand performance was not as successful in these trials. Thus, both the bulkier diethyl methylmalonate and benzylamine nucleophiles provided inferior results, and less reactive allylic acetates also performed poorly.

X-ray Structures. Not surprisingly, several of the second-generation ligands were shown to chelate on square-planar palladium(II) (Figures 8−10). The six-membered chelating rings again adopted a twist boat conformation. Whether sterically bulky or small, the sulfur substituent maintained a pseudoaxial orientation (Figures 8 and 9). Bite angles for the palladium complexes also remained fairly constant between 95 and 97°.

A crystal suitable for X-ray analysis was also obtained for the allyl complex by allowing ligand **24c** to react with 1,3-diphenypropenylpalladium(II) chloride followed by an anion exchange with silver hexafluoroantiminate (Figure 10).

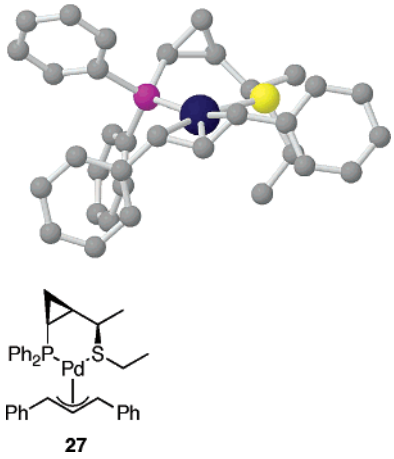

27

FIGURE 10. X-ray structure of [Pd(II)(1,3-diphenylallyl)-(**24c**)]SbF_6 (counterion omitted for clarity).

Solution-Phase Conformation. To determine if the solid-state configuration was the same as that in solution, complexes **26** and **27** were inspected by ^1H and ^{31}P NMR spectroscopy. Interestingly, while **26** showed only one ^{31}P

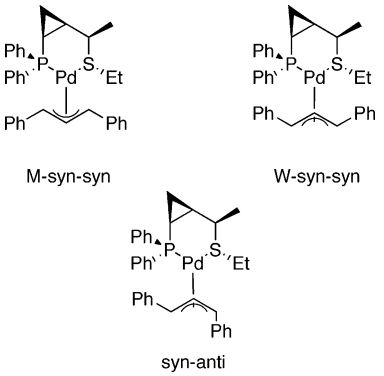

FIGURE 11. Possible allyl-palladium isomers.

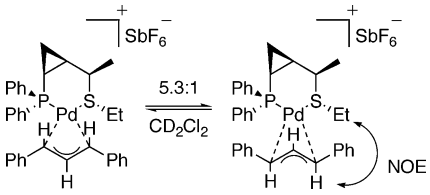

FIGURE 12. Interpretation of NOESY data in determining M- and W-isomers.

resonance, **27** existed as two isomers in a 5.3:1 ratio at room temperature in CD_2Cl_2. This suggests that sulfur inversion is negligible at room temperature, but that there is some equilibration between allyl conformations in the η^3-complex. Again, the lack of *S*-inversion is surprising because previous reports required large alkyl groups (e.g., *tert*-butyl) to prevent inversion (Figure 8).[11]

Of the several possible allyl isomers, COSY and NOESY data suggested that both isomers of **27** in solution have the syn-syn configuration, rather than the sterically unfavorable syn-anti (or anti-anti) structure (Figure 11).

In the observed NOESY spectrum, no NOE interactions between the allyl protons and the *S*-ethyl group were seen in the major isomer, suggesting that it is the M-isomer; the same diastereomer was observed in the solid state (Figure 12). Weak interactions were seen in the minor isomer, however, between a terminal allylic proton and the CH_3 protons on the *S*-ethyl group, suggesting that it is the opposite W-isomer. These findings are also consistent with reports in the literature.[11]

Mechanistic Considerations. These conclusions allow mechanistic predictions and comparison to observed products. Nucleophilic attack should occur at the carbon trans to the stronger σ-donating and π-accepting phosphorus atom according to the trans influence. Attack at this carbon on the M-isomer would give one enantiomer, while attack on the analogous carbon in the W-isomer would result in the opposite enantiomer (Scheme 5). Attack on the M-isomer should be fast in that it relieves steric strain between the allyl phenyl group and the *S*-ethyl substituent, while attack on the minor isomer would be slow owing to the steric strain generated in the transition state between the *S*-ethyl group and the allyl phenyl ring in the palladium(0)−olefin product. Curtin−Hammett kinetics appear to be operating in this system. Thus, interchange between the two allyl isomers must

SCHEME 5

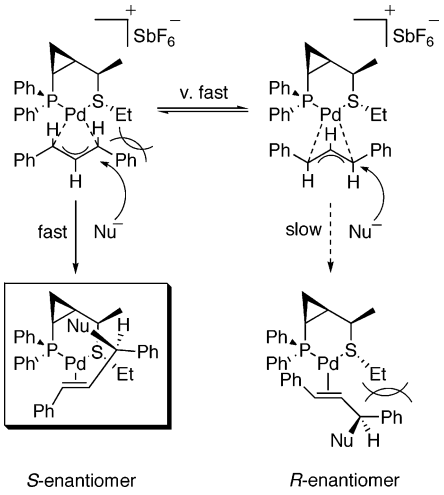

be quicker than either nucleophilic reaction, because the observed enantiomeric ratio of the product (91% ee, 21:1 er in CH_3CN) is greater than the solution-phase ratio of complex isomers (4.7:1 dr in CD_3CN).

The proposed mechanism predicts that an (*S*,*R*,*R*)-ligand (the enantiomer depicted in Figure 12) generates the (*S*)-enantiomer as the major product. This is in fact what is observed for ligand **24c** (based upon optical rotation measurements).

X-ray structures of complex **27** and the Evans ligand complex **28** allow structural comparisons that might reveal why the two catalyst systems, though sharing many similar features, still differ in the levels of observed enantioselectivity (Figures 13 and 14).[11]

A front-on comparison shows that in both complexes, the 1,3-diphenylallyl ligand is rotated slightly counterclockwise relative to the perpendicular ligand/metal plane. Quantitatively, in **27** the C1−Pd−C3 plane is 18.5° rotated from the P−Pd−S plane, while in **28** the difference is only 9.4°. Both catalyst systems have similar face-on/edge-on arrangements of the phenyl rings. The Pd−C1 and Pd−C3 bond lengths also are similar, though **28** shows a slightly stronger trans influence (Δ 0.11 Å vs Δ 0.09 Å).

A side-on comparison reveals similar tilts of the C1−C2−C3 ligand plane relative to the P−Pd−S plane, with complex **27** tilted 61.2° toward the face-on phenyl ring

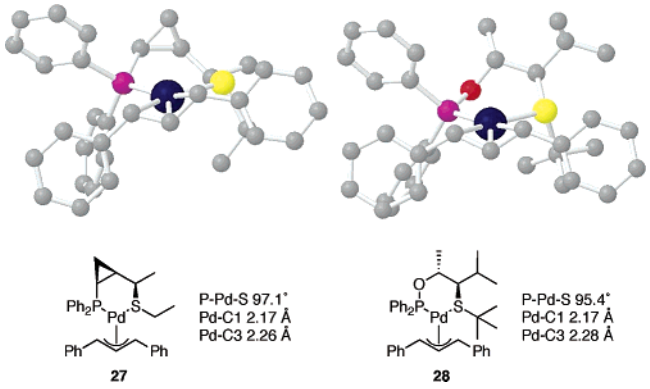

FIGURE 13. Front-on comparison of **27** and the Evans complex **28**.

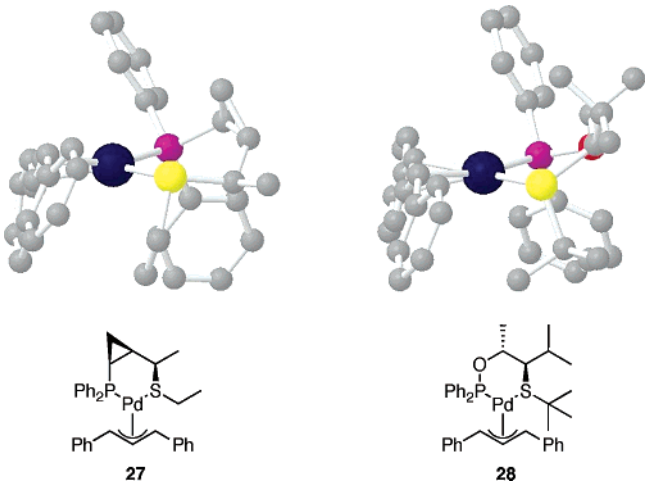

FIGURE 14. Side-on comparison of **27** and Evans complex **28**.

and the Evans system 61.9° toward the same direction (Figure 14). The complexes differ, however, in the orientation of the sulfur substituent: the ethyl group of complex **27** points toward the allyl ligand while the *tert*-butyl group of complex **28** points away from the allyl ligand. This is also revealed in the nonbonded distance between the first carbon off the sulfur and the first phenyl ring carbon cis to the sulfur atom: 3.52 Å in **27** versus 4.35 Å in **28**. The much shorter distance in complex **27** might explain why smaller R groups on the sulfide performed better; larger groups (e.g., *tert*-butyl) would cause severe steric congestion. Although we can only speculate, it may also explain the difference in the levels of enantioselectivity observed between the Evans ligand and the cyclopropyl series of ligands. Curiously, as the allylic carbon is rehybridizing in the transition structures leading to product, the *S*-Et group in **27** may provide more steric congestion than the *S*-*t*-Bu group of **28** simply due to its orientation. Thus, although in both systems the electronic effects favor alkylation at the site cis to the *S*-ligand on palladium, steric effects in the Evans systems at that same position are minimized relative to those of the cyclopropyl ligand motif, and thus higher enantioselectivities are observed.

Heck Reaction. To examine the reliability of the allylic alkylation reaction as a ligand benchmark, selected ligands were tested in the palladium-catalyzed intermolecular Heck reaction between phenyl triflate and 2,3-dihydrofuran (Table 4). Overall, most ligands gave ee values 20−30% lower in this asymmetric Heck reaction than when evaluated in the palladium-catalyzed AAA. Surprisingly, the best-performing ligand **12a** (91% optical purity) out-performed the previously successful ligand **24d**. The highest **A/B** ratios were obtained with the benzene/*i*-Pr_2NEt combination; other bases, such as Et_3N and K_2CO_3, always gave less selective results. Moreover, palladium sources other than $Pd_2(dba)_3$ generally gave a larger percentage of isomerization product **B**.

Rh-Catalyzed Hydrogenation. A few ligands were also tested in the rhodium-catalyzed hydrogenation of dehydroamino acids (Table 5). Higher pressures of hydrogen increased enantioselectivity while at the same time decreasing the rate of the reaction. Also, as the last entry clearly demonstrates, the pre-catalyst had to be synthesized beforehand and could not be formed in situ without greatly lowering the reaction rate.

TABLE 4. Results of Selected Ligands in Pd-Catalyzed Intermolecular Heck Reaction

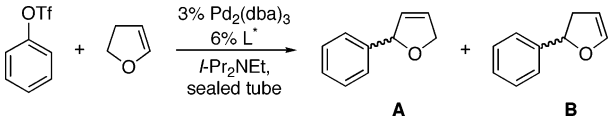

						ee, %	
L*	solvent	temp, °C	time, h	conv, %	**A/B**	**A**	**B**
1[a]	THF	70	20	99	0.05	8	7
1	C_6H_6	70	20	48	0.14	<5	
10a	THF	80	48	<5	~1	16	<5
10b	THF	70	48	99	8.0	36	45
12a[b]	C_6H_6	65	60	99	3.9	54	55
12a[b]	C_6H_6	65	60	93	10.6	63	43
12c	THF	70	48	81	2.6	17	12
trans-**12f**	THF	70	60	<5			
24d[a]	THF	60	48	99	2.6	55	36
24d[a]	THF	65	60	99	8.1	55	31
24d[a]	C_6H_6	70	60	99	9.7	50	19
24d[a,b]	C_6H_6	40	18	51	3.4	61	20
24d[a,c]	C_6H_6	40	18	17	10.7	55	
24d[a]	C_6H_6	40	18	28	11.2	52	
24d[a]	THF	65	60	57	10.8	52	28
24d[a,d]	THF	65	60	43	all B		0
24d[a,e]	THF	65	60	71	6.8	49	16

[a] Et_3N used as base. [b] $Pd(OAc)_2$ used as catalyst. [c] $Pd_2(dba)_3 \cdot CHCl_3$ used as catalyst. [d] 3 Å mol sieves added; Bu_4NCl (1 equiv) added. [e] K_2CO_3 used as base.

TABLE 5. Results of Various Ligands in Rh-Catalyzed Hydrogenation

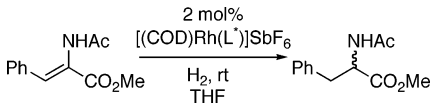

L+	pressure, psi	time, h	conv, %	ee, %
10b	100	42	27	5
12a	100	42	93	46
24d	14.7	48	99	41
24d	120	19	41	47
24d	200	18	19	47
24d[a]	100	18	99	45
24d[b]	100	18	7	

[a] MeOH used as solvent. [b] Catalyst formed in situ with Rh(COD)Cl and **24d**.

Conclusions

A new series of P/S ligands have been synthesized and evaluated in the palladium-catalyzed allylic alkylation reactions with moderate to good enantioselectivity. An X-ray crystal structure of the active catalyst was obtained. This, combined with NMR spectroscopic studies, was used to assign the major diastereomer in solution, which in turn was utilized to propose a mechanism for the enantioselectivity of the allylic alkylation. The ligand system was also compared to the Evans P/S catalyst system, a "gold standard" among this ligand class. Subtle structural differences were noted that may explain the rather dramatic differences in the performance of the two systems.

The scope of the best-performing ligand in this reaction was also evaluated in the palladium-catalyzed intermo-

lecular Heck reaction and the rhodium-catalyzed hydrogenation of dehydroamino acids, both with somewhat less successful results.

Experimental Section

See Supporting Information.

Acknowledgment. We thank the National Institutes of Health (NIGMS 48580) for their generous support and Johnson Matthey for a loan of the palladium catalysts used in this study. J.P.B. thanks Eli Lilly for a Graduate Fellowship.

Supporting Information Available: Experimental data, spectral characterization, and general procedures for asymmetric reactions; crystal data in CIF format. This material is available free of charge via the Internet at http://pubs.acs.org.

JO048782S